Photoelectron spectroscopy and density functional calculations of $Fe_nBO_2^-$ clusters

Yuan Feng, Hong-Guang Xu, Zeng-Guang Zhang, Zhen Gao, and Weijun Zheng[a)]
State Key Laboratory of Molecular Reaction Dynamics, Beijing National Laboratory for Molecular Science, Institute of Chemistry, Chinese Academy of Sciences, Beijing 100190, China

(Received 20 November 2009; accepted 6 January 2010; published online 19 February 2010)

We conducted a study of $Fe_nBO_2^-$ clusters by mass spectrometry and photoelectron spectroscopy. The vertical detachment energies and adiabatic detachment energies of these clusters were evaluated from their photoelectron spectra. We have also performed density-functional calculations of $Fe_nBO_2^-$ (n=1–5) clusters and determined their structures by comparison of theoretical calculations to experimental results. The studies show that BO_2 moiety still maintains its linear structure as the bare BO_2 cluster. BO_2 behaves as a superhalogen. Analysis of molecular orbitals reveals that the highest occupied molecular orbitals of $Fe_nBO_2^-$ clusters are mainly localized on the Fe_n units. © *2010 American Institute of Physics*. [doi:10.1063/1.3299290]

I. INTRODUCTION

In the past decades, much attention has been paid to investigate, experimentally[1–3] and theoretically[4–9] the structures of boron and boron oxides because of their applications in superconduction,[10–12] electronic device, and aerospace industry.[13–16] Very recently, anion photoelectron spectroscopy (PES)[17,18] and theoretical[19,20] investigation of small boron oxides show that BO can maintain its chemical integrity as a key structural unit and behaves like a monovalent unit in its bonding to other atoms.

Boron oxides can react efficiently with iron, and the specialty is extensively used in metallurgy. For example, the addition of boron oxide into magnesium alloy during the production process can greatly reduce the iron impurity.[21] In order to utilize the boron mineral resource more efficiently, the new pyrometallurgical methods were developed to separate iron and boron oxides from low grade ludwigite and vonsenite minerals.[22] Among the interactions between boron oxides and iron, the interactions between BO_2 and iron clusters are much more concerned. The BO_2 radical is a prototypical linear Renner–Teller molecule, and its spectroscopy has been studied extensively in the past decades.[23–40] Due to the involvement of Renner–Teller effect, spin-orbit coupling, Fermi resonance, and anharmonicities, the spectroscopy of BO_2 is very complex and cannot be interpreted successfully with only simple theoretical treatments. For this reason, BO_2 has been considered as an ideal molecule for the theoretical study of triatomic molecules. In addition, BO_2 is only one electron short to electronic shell closing and has high electron affinity (EA), 4.46 eV,[41] larger than that of halogen atoms, so that BO_2 can be considered as a superhalogen.[42,43] Here we report a study of $Fe_nBO_2^-$ (n=1–10) by PES combined with the calculations performed using density-functional theory (DFT) to understand the interactions between BO_2 and iron clusters as well as the superhalogen properties of BO_2.

II. EXPERIMENTAL AND COMPUTATIONAL METHODS

A. Experimental

The experiments were conducted on a home-built apparatus consisting of a time-of-flight (TOF) mass spectrometer and a magnetic-bottle photoelectron spectrometer, which has been described elsewhere.[44] Briefly, the $Fe_nBO_2^-$ (n=1–10) cluster anions were produced in a laser vaporization source by ablating a rotating, translating B/Fe alloy target (13 mm diameter, Fe/B mole ratio of 50:1) with the second harmonic (532 nm) light pulses of a Nd:YAG (yttrium aluminum garnet) laser, while helium gas with 4 atm was allowed to expand through a pulsed valve over the alloy target. The residual oxygen on the target surface was sufficient to produce abundant $Fe_nBO_2^-$ clusters, so no additional oxygen was introduced into the source. The cluster anions were mass analyzed by the TOF mass spectrometer. The $Fe_nBO_2^-$ (n=1–10) clusters were each mass selected and decelerated before being photodetached. The photodetachment of the selected cluster anions was performed by the fourth harmonic (266 nm, 4.661 eV/photon) of the second Nd:YAG laser, and the resulted electrons were energy analyzed by the magnetic-bottle photoelectron spectrometer. The PES spectra were calibrated using the known spectrum of Cu^-. The instrumental resolution was approximately 40 meV for electrons with 1 eV kinetic energy.

B. Computational methods

The calculations of $Fe_nBO_2^-$ (n=1–5) clusters were performed using density functional theory at B3LYP/6-311+g(d) level implemented in GAUSSIAN03 program package.[45] Glukhovtsev *et al.*[46] reported the excellent performance of B3LYP functional for iron-containing complexes on geometries, bond dissociation energies, ionization energies com-

a)Author to whom correspondence should be addressed. Electronic mail: zhengwj@iccas.ac.cn. Tel.: +86 10 62635054. FAX: +86 10 62563167.

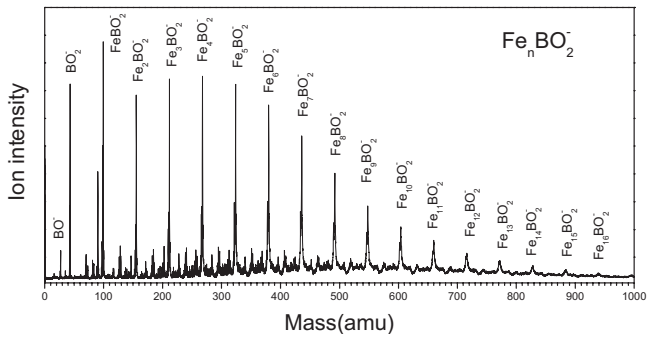

FIG. 1. Mass spectrum of $Fe_nBO_2^-$ cluster anions.

paring with the experimental and higher level computational data. This method is expected to be accurate enough for determining the structural and chemical properties of first-row transition metal containing species. We have tested different methods and basis sets on some small molecules such as Fe_2, FeO, BO, B_2, and O_2, and compared the results with the experiments in the literature (Table S1, supporting information).[47] The results obtained using B3LYP functional with 6-311+g(d) basis set have the best agreement with the experimental data in the literature. Thus, B3LYP/6-311 +g(d) is used in this work.

The structures of $Fe_nBO_2^-$ (n=1–5) and their corresponding neutrals were determined by optimizing structures at several different multiplicities using several different initial geometries. No symmetry constraint was employed during the optimizations, and the calculated energies were corrected by the zero-point vibrational energies. Harmonic vibrational frequencies were calculated to make sure that the structures correspond to real local minima. The vertical electron detachment energies were calculated as the energy differences between the neutrals and anions at the geometry of the anionic species. Note that the neutral energy was calculated at the geometry of the corresponding anion for each possible spin state governed by Δ (spin multiplicity)$=\pm 1$.

III. EXPERIMENTAL RESULTS

Figure 1 shows a typical, reproducible mass spectrum of cluster anions generated in the experiments. It can be seen that the major mass peaks are those of $Fe_nBO_2^-$ cluster anions, and the mass peaks of $Fe_nBO_2^-$ with n=1–16 were presented clearly. The assignments of the mass peaks were confirmed by analyzing the isotope abundances of $Fe_nBO_2^-$ clusters. For example, by considering the nature isotope abundances of iron and boron, $FeBO_2^-$ should have isotopic peaks at mass numbers of 96, 97, 98, 99, 100, and 101 amu with abundances of approximately 1.2%, 4.6%, 18.2%, 73.6%, 1.9%, and 0.5%, respectively. The mass peaks in our experiments are in agreement with the isotope distributions.

The photoelectron spectra of $Fe_nBO_2^-$ with n=1–10 generated with 266 nm photons are shown in Fig. 2. Each of these PES spectra represents the transitions from the ground state of the anion to the ground or excited states of corresponding neutral. The vertical detachment energies (VDEs) and the adiabatic detachment energies (ADEs) of the cluster anions estimated from their photoelectron spectra were listed

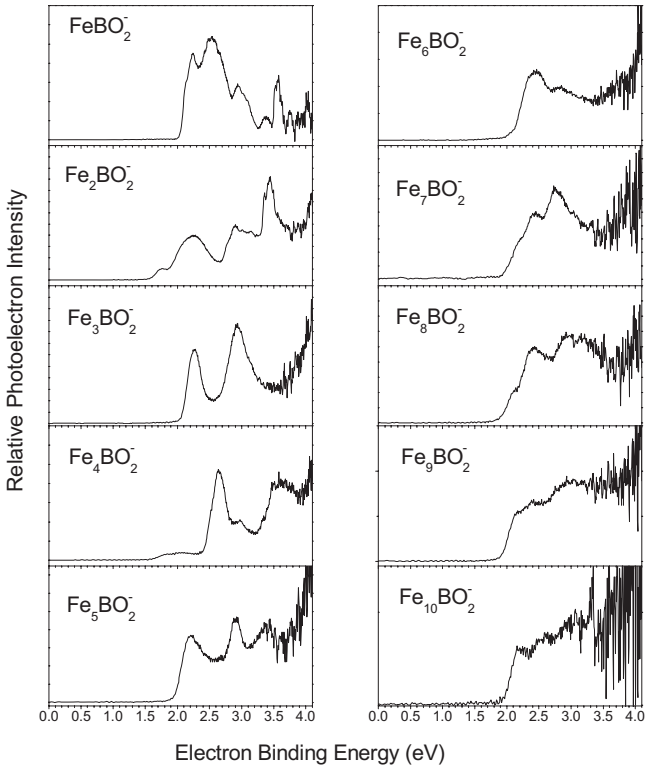

FIG. 2. Photoelectron spectra of $Fe_nBO_2^-$ (n=1–10) clusters recorded with 266 nm photons.

in Table I. To account for the broadening of the PES spectrum due to instrumental resolution, the ADE was calculated by adding the half value of instrumental resolution to the onset of the first peak in the spectrum. The onset of the first peak was found by drawing a straight line along the leading edge of that peak to cross the baseline of the spectrum. It is supposed that the ADE of the cluster anion is equal to the EA of the corresponding neutral.

In comparison of the values shown in Table I, we can see that the ADEs, i.e., the EAs of the corresponding neutrals, Fe_nBO_2, do not change much when the number of the iron atoms increases from 1 to 10, except the EAs of Fe_2BO_2 and Fe_4BO_2 are slightly lower than those of the others. The EAs of Fe_nBO_2 are in the range between 1.6 and 2.2 eV much lower than that of BO_2.

TABLE I. Experimentally observed VDEs and ADEs from the photoelectron spectra of $Fe_nBO_2^-$ (n=1–10).

Cluster	ADE (eV)	VDE (eV)
$FeBO_2^-$	2.04(8)[a]	2.28(8)
$Fe_2BO_2^-$	1.60(8)	1.79(8)
$Fe_3BO_2^-$	2.07(8)	2.31(8)
$Fe_4BO_2^-$	1.6(1)	1.9(1)
$Fe_5BO_2^-$	1.98(8)	2.28(8)
$Fe_6BO_2^-$	2.14(8)	2.45(8)
$Fe_7BO_2^-$	1.97(8)	2.22(8)
$Fe_8BO_2^-$	1.90(8)	2.12(8)
$Fe_9BO_2^-$	1.93(8)	2.18(8)
$Fe_{10}BO_2^-$	1.98(8)	2.13(8)

[a]The numbers in parentheses indicate the uncertainties in the last digit.

The PES spectrum of $FeBO_2^-$ is presented with six features centered at 2.23, 2.54, 2.94, 3.38, 3.57, and 3.75 eV, respectively. For the PES spectrum of $Fe_2BO_2^-$, a small peak centered at 1.73 eV, a broad feature centered at 2.24 eV, a dominating sharp peak at 3.44 eV, and three unresolved peaks at about 2.90, 3.02, and 3.15 eV are observed. Two strong peaks centered at 2.26 and 2.93 eV are evident in the PES spectrum of $Fe_3BO_2^-$. The PES spectrum of $Fe_4BO_2^-$ contains a strong peak centered at 2.64 eV and a small one at 2.97 eV followed by an unresolved broad feature at 3.57 eV, and in addition, a small and broad feature centered at 2.03 eV is also observed in the spectrum of $Fe_4BO_2^-$. The PES spectrum of $Fe_5BO_2^-$ has three major peaks centered at 2.21, 2.91, and 3.40 eV followed by an unresolved feature at higher binding energy.

Two broad features centered at 2.47 and 2.83 eV are distinguishable in the PES spectrum of $Fe_6BO_2^-$. Two major features centered at 2.41 and 2.73 eV and a small shoulder at 2.19 eV are evident in the PES spectrum of $Fe_7BO_2^-$. The PES spectrum of $Fe_8BO_2^-$ has a small shoulder at 2.10 eV and a broad peak at approximately 2.43 eV, followed by an unresolved broad feature at higher binding energy. The PES spectra of $Fe_9BO_2^-$ and $Fe_{10}BO_2^-$ are not well resolved at the level of the instrumental resolution.

IV. THEORETICAL RESULTS AND DISCUSSION

The optimized geometries of the low-lying isomers of $Fe_nBO_2^-$ (n=1–5) clusters obtained with DFT calculations are presented in Fig. 3 with the most stable structures on the left. The most stable structures of $Fe_nBO_2^-$ (n=1–5) clusters are characterized by an iron cluster attaching to one end of linear BO_2. The calculated structures shown in Fig. 3 are all planar structures. We have also tried many other initial structures, such as to insert Fe atom between O and B atoms and to attach Fe atom directly to B atom; however, those tried geometries are unstable compared with the structures shown in Fig. 3. The fact indicates that the BO_2 is a stable unit.

The structures of the neutral clusters Fe_nBO_2 (n=1–5) were also optimized using their corresponding anion structures in Fig. 3 as initial structures. The most stable structures of Fe_nBO_2 neutrals are presented in Fig. 4. Based on the energy differences between the neutrals and anions, we calculated the ADEs of these isomers. The calculated VDEs and ADEs of $Fe_nBO_2^-$ (n=1–5) clusters are listed in Table II, in which the experimental values are also presented. It is shown that the theoretical VDEs and ADEs of the most stable structures, labeled as "nA" (n=1–5) in Table II, are in agreement with the experimental values.

For $FeBO_2^-$, the structure with the lowest energy is 1A, which is a linear structure in quintet state with Fe atom attached to one end of BO_2, and the theoretical VDE and ADE of 1A shown in Table II are in agreement with the experimental values. The other isomers of $FeBO_2^-$ such as 1B and 1C are higher in energy, and also their theoretical VDEs are very different from the experimental values. Therefore, it is suggested that only the structure 1A contributes to the experimental PES spectrum.

There are two stable structures with little difference in energy for $Fe_2BO_2^-$ (isomers 2A and 2B in Fig. 3). Isomer 2A is formed by attaching an Fe atom to $FeBO_2^-$ via Fe—Fe bond, and isomer 2B has C_{2v} symmetry with both Fe atoms bond directly to one oxygen atom in BO_2. The calculated VDEs of the two isomers (1.69 eV for 2A and 1.73 eV for 2B) are in agreement with the experiment measurement (1.79 eV), and the calculated ADEs of 2A and 2B are also close to the experimental values. For the above reason, the assignment should be that both isomers 2A and 2B exist in the experiments. The Fe—Fe bond length in $Fe_2BO_2^-$ is about 2.13 Å, which is very close to the Fe—Fe bond in the pure Fe_2^- cluster (2.10 Å).[48]

It was known that the most stable geometry of Fe_3^- is an equilateral triangular structure with a bond length of 2.10 Å.[49,50] For $Fe_3BO_2^-$ the lowest-energy structure might

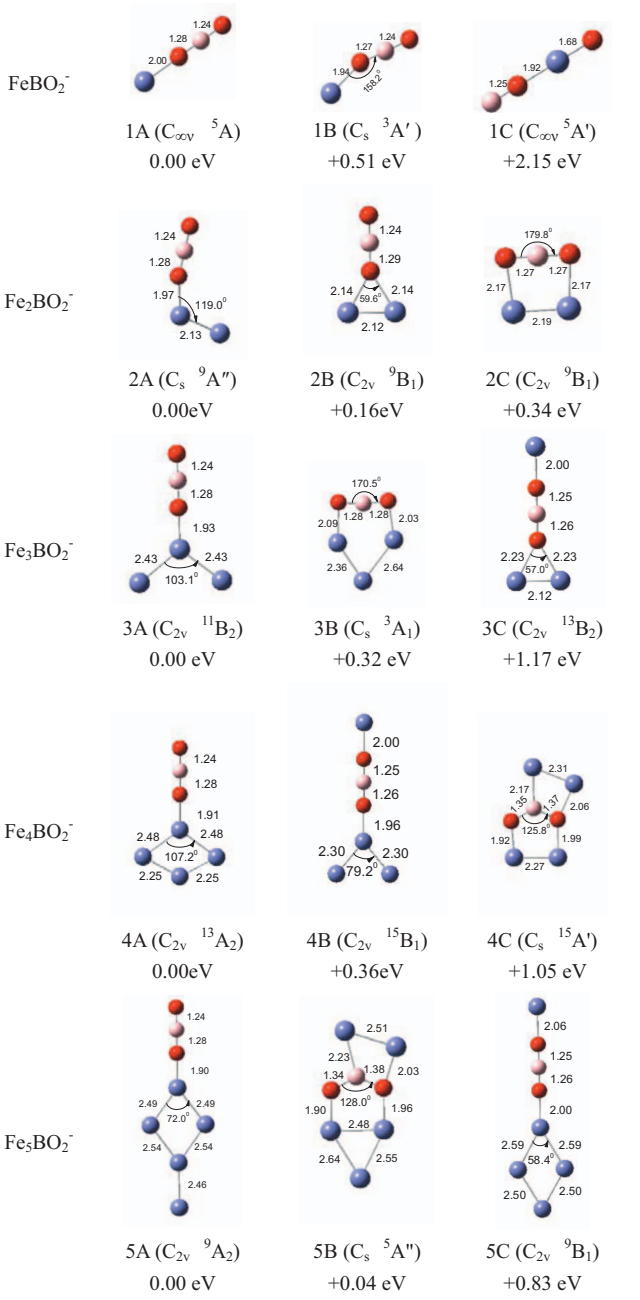

FIG. 3. Optimized geometries of the low-lying isomers of $Fe_nBO_2^-$ (n=1–5) clusters.

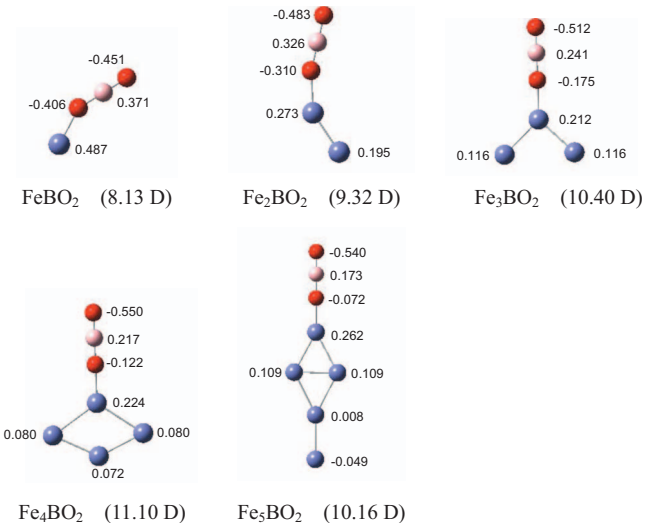

FIG. 4. Milliken atomic charges and dipole moments of Fe_nBO_2 (n=1–5) neutral clusters. (The numbers in the parentheses are the dipole moments.)

be obtained by adding the linear BO_2 to the Fe_3 with the C_{2v} symmetry. The Fe_3 in $Fe_3BO_2^-$ is distorted to an isosceles triangle, and the linear BO_2 attaches to the vertex Fe atom with the Fe—Fe distance of 2.43 Å and an angle of 103.1° shown in Fig. 3 (3A). The theoretical VDE (2.31 eV) and ADE (2.18 eV) of isomer 3A are all close to the experimental VDE of 2.31 eV and ADE of 2.07 eV. The theoretical VDEs of isomers 3B and 3C are 1.28 and 2.15 eV, respectively, much deviated from the experimental value. That implies that only isomer 3A exists in the experiments.

The most stable structure of $Fe_4BO_2^-$ is found to be isomer 4A, and the calculated VDE of isomer 4A is 1.91 eV, which is in agreement with the experiment value. The calculated ADE of isomer 4A is 1.82 eV, which is slightly higher than the experimental value of 1.6 eV. The energies of isomers 4B and 4C are higher than that of isomer 4A by 0.36 and 1.05 eV, respectively. The VDEs of isomers 4B and 4C are much higher than the experimental value. Thus, isomer 4A is probably the species that contributed to the experimental PES spectrum of $Fe_4BO_2^-$. In the structure 4A of $Fe_4BO_2^-$, Fe_4 forms a planar rhombus, and the Fe—Fe distances are 2.25 and 2.48 Å, which are very different from the structure of the pure Fe_4, which has a tetrahedron structure with a bond length of 2.22 Å.[49,50]

For $Fe_5BO_2^-$, the most stable structure is 5A with C_{2v} symmetry. The structure 5A can be obtained by adding one Fe atom to $Fe_4BO_2^-$ with Fe—Fe bond. The calculated VDE and ADE of the structure 5A are 2.38 and 1.99 eV, respectively, which are consistent with the experimental values in Table II. Although the energy of isomer 5B is higher than isomer 5A by only 0.04 eV, its VDE is calculated to be 5.04 eV, much different from the experimental value. The calculated VDE (2.32 eV) of isomer 5C is close to the experimental value, but the energy of isomer 5C is much higher than that of isomer 5A. So the existence of isomers 5B and 5C in the experiments can be excluded. In the pure Fe_5^-, symmetric bipyramid is found to be the most stable structure,[49] but in $Fe_5BO_2^-$ cluster, Fe_5 possesses a planar structure, and the Fe—Fe distance is in the range of 2.46–2.54 Å.

Figure 3 (left column) shows that the most stable structures of $Fe_nBO_2^-$ (n=1–5) are all planar structures. They can all be considered as linear BO_2 attaching to Fe_n via Fe—O bond. It is noticed that the structure of BO_2 unit and the B—O bond length in $Fe_nBO_2^-$ are nearly identical to those in the bare BO_2^-. Wang and co-workers[41] performed PES and theoretical investigation on BO^- and BO_2^- clusters. Their studies confirmed that the bonding in BO^- can be viewed approximately as a B≡O triple bond, and the bonding in BO_2^- can be described as two B=O double bonds with the bond length of 1.27 Å and BO_2^- has a linear geometry. For $Fe_nBO_2^-$ clusters, BO_2 holds a linear geometry with one oxygen atom attaching to Fe_n. The two B—O bond

TABLE II. Relative energies of the low energy isomers of $Fe_nBO_2^-$ (n=1–5) as well as their VDEs and ADEs obtained by DFT calculations.

Isomers		ΔE (eV)	Symmetry	State	ADE (eV)		VDE (eV)	
					Theor.	Expt.	Theor.	Expt.
$FeBO_2^-$	1A	0.00	$C_{\infty v}$	^5A	1.92	2.04	2.13	2.28
	1B	0.51	C_s	$^3A'$	1.41		1.52	
	1C	2.15	$C_{\infty v}$	$^5A'$	2.96		3.00	
$Fe_2BO_2^-$	2A	0.00	C_s	$^9A''$	1.50	1.60	1.69	1.79
	2B	0.16	C_{2v}	$^9B_1$	1.65		1.73	
	2C	0.34	C_{2v}	$^9B_1$	2.11		2.31	
$Fe_3BO_2^-$	3A	0.00	C_{2v}	$^{11}B_2$	2.18	2.07	2.31	2.31
	3B	0.32	C_s	$^3A_1$	1.22		1.28	
	3C	1.17	C_{2v}	$^{13}B_2$	1.79		2.15	
$Fe_4BO_2^-$	4A	0.00	C_{2v}	$^{13}A_2$	1.82	1.6	1.91	1.9
	4B	0.36	C_{2v}	$^{15}B_1$	3.14		3.40	
	4C	1.05	C_s	$^{15}A'$	2.32		2.66	
$Fe_5BO_2^-$	5A	0.00	C_{2v}	$^9A_2$	1.99	1.98	2.38	2.28
	5B	0.04	C_s	$^5A''$	3.45		5.04	
	5C	0.83	C_{2v}	$^9B_1$	2.09		2.32	

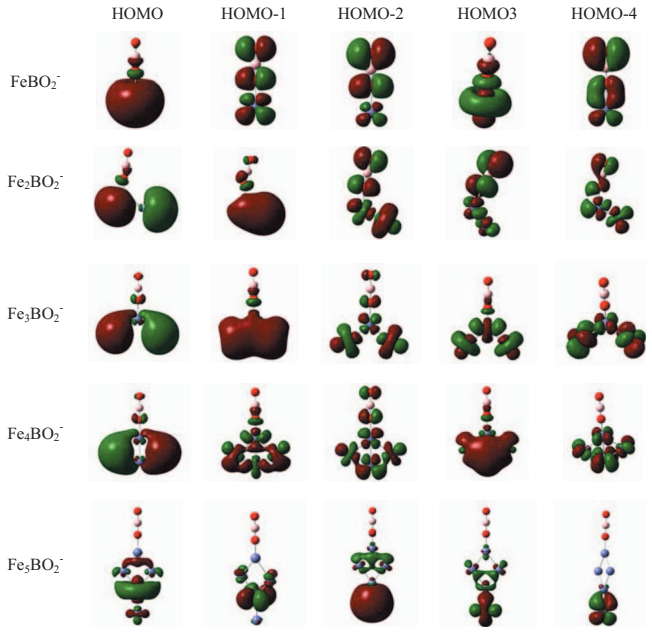

FIG. 5. Diagrams of the molecule orbitals of $Fe_nBO_2^-$ (n=1–5).

lengths are 1.24 and 1.28 Å, respectively. The above suggests that the BO_2 can maintain its structure integrity when it interacts with iron clusters.

As it has been proposed by theoretical calculations, BO_2 can be considered as a superhalogen because of its high EA and special electronic property.[42,43] Therefore, it is interesting to compare the Fe—O distance in $Fe_nBO_2^-$ clusters with Fe—Cl in $FeCl_2$.[51,52] The Fe—Cl bond length in $FeCl_2$ has been reported to be 2.132 Å.[51] We found that the Fe—(OBO) distances in $Fe_nBO_2^-$ are between 1.90 and 2.00 Å, slightly shorter than the Fe—Cl bond length. PES studies[41] show that the EA of BO_2 is much higher than the EA of Cl atom, indicating that BO_2 has stronger electronegativity than chlorine. This fact probably can explain why the Fe—(OBO) distance is shorter than Fe—Cl bond length. These results support the theoretical prediction of superhalogen BO_2.

In Fig. 3, the calculated bond length of Fe—Fe in $Fe_nBO_2^-$ clusters is in the range of 2.12–2.64 Å, which is longer than the experiment values obtained in argon[53] and neon[54] matrices, 1.87 and 2.02 Å, respectively, but shorter than the nearest neighbor distance (2.87 Å) (Ref. 55) in metallic iron. The fact indicates that strong interactions between the iron atoms exist in $Fe_nBO_2^-$ clusters.

To investigate the bonding in $Fe_nBO_2^-$ (n=1–5) clusters, we examined the electron densities of their molecular orbitals. The electron distributions of the first five orbitals of the lowest-energy configurations of $Fe_nBO_2^-$ (n=1–5) are plotted in Fig. 5. We can see from Fig. 5 that the highest occupied molecular orbitals (HOMOs) of these clusters are mainly located on the Fe_n units. That indicates the PES features in our spectra are mostly contributed by the 3d and 4s electrons of Fe, which is consistent with the complex PES features observed in our experiments.

The most stable geometries of Fe_nBO_2 neutral as well as their Mulliken populations are shown in Fig. 4. For Fe_nBO_2 clusters, the charge of Fe_n is positive while the charge of BO_2 is negative with the distributions $(Fe)^{0.49+}(OBO)^{0.49-}$, $(Fe_2)^{0.47+}(OBO)^{0.47-}$, $(Fe_3)^{0.45+}(OBO)^{0.45-}$, $(Fe_4)^{0.46+}(OBO)^{0.46-}$, and $(Fe_5)^{0.44+}(OBO)^{0.44-}$. The charges always transfer from Fe_n to BO_2, indicating that the electronegativity of BO_2 is larger than that of Fe_n. BO_2 acts as an electron acceptor in all Fe_nBO_2 clusters, and gets electron to form a close shell structure. It is worth mentioning that the Fe_nBO_2 (n=1–5) neutral clusters have fairly larger dipole moments scaled from 8.13 to 11.10 D. Their dipole moments are very similar to those of typical ionic compounds, such as NaCl (9.0 D), KCl (10.3 D), NaBr (9.1 D), and KBr (10.6 D). This probably is owing to the superhalogen property of BO_2. The analysis of the Mulliken populations (Fig. S1, supporting information)[47] and the HOMOs of $Fe_nBO_2^-$ cluster anions shows that the excess electron mainly localizes on the Fe_n units, the positive pole of the dipole, since it is repulsed by the negative pole.

Finally, the magnetic properties of $Fe_nBO_2^-$ clusters are commented. Magnetism is an important property of iron clusters, which is closely related to their electronic structures. The magnetic properties of the pure iron clusters have been well studied and they are all shown to be magnetic.[49,56–59] The evolution of the magnetic behavior with addition of BO_2 to the pure Fe_n clusters can be revealed by the unpaired electrons. From Fig. 3, it can be seen that the unpaired electrons of $Fe_nBO_2^-$ are 4, 8, 10, 12, and 8, respectively, for n=1–5, while the corresponding values for the pure Fe_n^- clusters are 3 6, 8, 10, and 12.[48,49,60] Clearly, the magnetic moments of Fe_n clusters have not been quenched by BO_2.

V. CONCLUSION

$Fe_nBO_2^-$ cluster anions were generated by laser ablation on a Fe/B alloy target and were mass analyzed with a TOF mass spectrometer. The photoelectron spectra of $Fe_nBO_2^-$ (n=1–10) cluster anions were measured with a magnetic-bottle photoelectron spectrometer. Density functional calculations were conducted to elucidate the structures of $Fe_nBO_2^-$ (n=1–5) clusters and their electronic properties. We find that $FeBO_2^-$ has a linear structure, and the other $Fe_nBO_2^-$ (n=2–5) clusters prefer to form planar structures with a Fe_n cluster attached to one end of BO_2. The BO_2 unit still maintains its linear structure similar to the isolated BO_2 molecule. BO_2 radical behaves as a superhalogen. The magnetic properties of iron clusters are only slightly affected by BO_2.

[1] A. P. Sergeeva, D. Y. Zubarev, H. J. Zhai, A. I. Boldyrev, and L. S. Wang, J. Am. Chem. Soc. **130**, 7244 (2008).
[2] A. N. Alexandrova, A. I. Boldyrev, H.-J. Zhai, and L.-S. Wang, J. Phys. Chem. A **108**, 3509 (2004).
[3] B. Kiran, S. Bulusu, H. J. Zhai, S. Yoo, X. C. Zeng, and L. S. Wang, Proc. Natl. Acad. Sci. U.S.A. **102**, 961 (2005).
[4] A. K. Ray, I. A. Howard, and K. M. Kanal, Phys. Rev. B **45**, 14247 (1992).
[5] S. H. Bauer, Chem. Rev. (Washington, D.C.) **96**, 1907 (1996).
[6] I. Boustani, Phys. Rev. B **55**, 16426 (1997).
[7] L. M. Yang, N. Wang, Y. H. Ding, and C. C. Sun, J. Phys. Chem. A **111**, 9122 (2007).
[8] M. L. Drummond, V. Meunier, and B. G. Sumpter, J. Phys. Chem. A **111**, 6539 (2007).

[9] W. Z. Yao, J. C. Guo, H. G. Lu, and S. D. Lit, J. Phys. Chem. A **113**, 2561 (2009).
[10] J. P. Goss and P. R. Briddon, Phys. Rev. B **73**, 085204 (2006).
[11] Y. Zhou and J. Zhi, Talanta **79**, 1189 (2009).
[12] D. B. Luo, L. Z. Wu, and J. F. Zhi, ACS Nano **3**, 2121 (2009).
[13] T. Hasegawa, Y. Ide, T. Nagatomo, T. Otagiri, R. Ide, and T. Odagiri, Patent Nos. WO2009041166-A1 and JP2009088089-A (2 April 2009).
[14] Y. L. Rao and S. N. Wang, Inorg. Chem. **48**, 7698 (2009).
[15] G. Q. Li, Appl. Phys. Lett. **94**, 3 (2009).
[16] Y. Cui, F. H. Li, Z. H. Lu, and S. N. Wang, Dalton Trans. **25**, 2634 (2007).
[17] S. D. Li, H. J. Zhai, and L. S. Wang, J. Am. Chem. Soc. **130**, 2573 (2008).
[18] H. J. Zhai, S. D. Li, and L. S. Wang, J. Am. Chem. Soc. **129**, 9254 (2007).
[19] T. B. Tai and M. T. Nguyen, Chem. Phys. Lett. **483**, 35 (2009).
[20] M. T. Nguyen, M. H. Matus, V. T. Ngan, D. J. Grant, and D. A. Dixon, J. Phys. Chem. A **113**, 4895 (2009).
[21] H. T. Gao, G. H. Wu, W. J. Ding, and Y. P. Zhu, Foundry **53**, 797 (2004).
[22] H. T. Cai and J. L. Zhang, Iron and Steel **43**, 31 (2008).
[23] J. V. Ortiz, J. Phys. Chem. A **99**, 6727 (1993).
[24] A. Sommer, M. J. Linevsky, D. E. Mann, and D. White, J. Chem. Phys. **38**, 87 (1963).
[25] D. E. Jensen, J. Chem. Phys. **52**, 3305 (1970).
[26] T. R. Burkholder and L. Andrews, J. Chem. Phys. **95**, 8697 (1991).
[27] V. G. Zakrzewski and A. I. Boldyrev, J. Chem. Phys. **93**, 657 (1990).
[28] J. R. Chow, R. A. Beaudet, W. Schulz, K. Weyer, and H. Walther, Chem. Phys. **140**, 307 (1990).
[29] A. G. Maki, J. B. Burkholder, A. Sinha, and C. J. Howard, J. Mol. Spectrosc. **130**, 238 (1988).
[30] K. Kawaguchi and E. Hirota, J. Mol. Spectrosc. **116**, 450 (1986).
[31] P. Császár, W. Kosmus, and Y. N. Panchenko, Chem. Phys. Lett. **129**, 282 (1986).
[32] V. Saraswathy, J. J. Diamond, and G. A. Segal, J. Phys. Chem. **87**, 718 (1983).
[33] K. G. Weyer, R. A. Beaudet, R. Straubinger, and H. Walther, Chem. Phys. **47**, 171 (1980).
[34] M. A. A. Clyne and M. C. Heaven, Chem. Phys. **51**, 299 (1980).
[35] R. S. Lowe, H. Gerhardt, W. Dillenschneider, R. F. Curl, and F. K. Tittel, J. Chem. Phys. **70**, 42 (1979).
[36] A. Fried and C. W. Mathews, Chem. Phys. Lett. **52**, 363 (1977).
[37] R. N. Dixon, D. Field, and M. Noble, Chem. Phys. Lett. **50**, 1 (1977).
[38] D. K. Russell, M. Kroll, D. A. Dows, and R. A. Beaudet, Chem. Phys. Lett. **20**, 153 (1973).
[39] J. V. Ortiz, J. Chem. Phys. **99**, 6727 (1993).
[40] J. Agreiter, M. Lorenz, A. M. Smith, and V. E. Bondybey, Chem. Phys. **224**, 301 (1997).
[41] H. J. Zhai, L. M. Wang, S. D. Li, and L. S. Wang, J. Phys. Chem. A **111**, 1030 (2007).
[42] G. L. Gutsev and A. I. Boldyrev, Chem. Phys. **56**, 277 (1981).
[43] C. George, F. Mayne, and I. Prigogine, Adv. Chem. Phys. **61**, 223 (1985).
[44] H.-G. Xu, Z.-G. Zhang, Y. Feng, J. Yuan, Y. Zhao, and W. Zheng, Chem. Phys. Lett. **487**, 204 (2010).
[45] M. J. Frisch, G. W. Trucks, H. B. Schlegel *et al.*, GAUSSIAN03, Revision B.04, Gaussian, Inc., Pittsburgh, PA, 2003.
[46] M. N. Glukhovtsev, R. D. Bach, and C. J. Nagel, J. Phys. Chem. A **101**, 316 (1997).
[47] See supplementary material at http://dx.doi.org/10.1063/1.3299290 for the test results of different computational methods and the Milliken atomic charges of the most stable $Fe_nBO_2^-$ (n=1–5) clusters.
[48] D. G. Leopold and W. C. Lineberger, J. Chem. Phys. **85**, 51 (1986).
[49] L. S. Wang, H. S. Cheng, and J. W. Fan, J. Chem. Phys. **102**, 9480 (1995).
[50] M. Castro and D. R. Salahub, Phys. Rev. B **47**, 10955 (1993).
[51] P. J. Hodges, J. M. Brown, and S. H. Ashworth, J. Mol. Spectrosc. **237**, 205 (2006).
[52] M. Hargittai, N. Y. Subbotina, and M. Kolonits, J. Chem. Phys. **94**, 7278 (1991).
[53] P. A. Montano and G. K. Shenoy, Solid State Commun. **35**, 53 (1980).
[54] H. Purdum, P. A. Montano, G. K. Shenoy, and T. Morrison, Phys. Rev. B **25**, 4412 (1982).
[55] R. W. G. Wyckoff, *Crystal Structures*, 2nd ed. (Interscience, New York, 1963).
[56] S. Q. Yu, S. G. Chen, W. W. Zhang, L. H. Yu, and Y. S. Yin, Chem. Phys. Lett. **446**, 217 (2007).
[57] S. Li, M. M. G. Alemany, and J. R. Chelikowsky, Phys. Rev. B **73**, 233404 (2006).
[58] C. Kohler, G. Seifert, and T. Frauenheim, Chem. Phys. **309**, 23 (2005).
[59] G. L. Gutsev and C. W. Bauschlicher, J. Phys. Chem. A **107**, 7013 (2003).
[60] P. C. Engelking and W. C. Lineberger, Phys. Rev. A **19**, 149 (1979).